Synthesis and Electronic Properties of New Photoluminescent Platinum-Containing Polyynes with 9,9-Dihexylfluorene and 9-Butylcarbazole Units

Wai-Yeung Wong,* Guo-Liang Lu, Ka-Ho Choi, and Jian-Xin Shi

Department of Chemistry, Hong Kong Baptist University, Waterloo Road, Kowloon Tong, Hong Kong, P. R. China

Received October 1, 2001; Revised Manuscript Received February 5, 2002

ABSTRACT: Soluble, thermally stable, and easily processable platinum(II) polyyne polymers *trans*-[−Pt(PBu_3)$_2$C≡CRC≡C−]$_n$ (R = 9,9-dihexylfluorene-2,7-diyl or 9-butylcarbazole-3,6-diyl) have been prepared in good yields by CuI-catalyzed polymerization involving the dehydrohalogenating coupling of *trans*-[$PtCl_2(PBu_3)_2$] and HC≡CRC≡CH. We report their optical absorption and photoluminescence spectra and compare the results with the monomeric model complexes *trans*-[Pt(Ph)(PEt_3)$_2$C≡CRC≡CPt(Ph)-(PEt_3)$_2$] and other fluorene derivatives exhibiting different degrees of electronic conjugation. The regiochemical structure of the polymers has been ascertained by single-crystal X-ray analysis on the carbazole-linked model compound. With decreasing conjugation, the optical gap as well as intersystem crossing from the singlet excited state to the triplet excited state is increased. In both systems, our studies indicate that the S_1 singlet excited state extends over more than a repeat unit while the T_1 triplet state remains localized to less than one repeat unit. The photoconducting properties of these platinum polyynes are discussed.

Introduction

In the past few decades, great efforts have been devoted to the design and synthesis of light-emitting organic polymers in the scientific community because of their potential applications in optoelectronic devices[1] such as light-emitting diodes (LEDs),[2] lasers,[3] and photocells.[4,5] An identified problem in organic LEDs is the ratio of 3:1 for the generation of (nonemissive) triplet to (emissive) singlet excitons.[6] In light of this drawback, conjugated polymers containing transition-metal atoms such as platinum in the main chain have been widely studied by us and others as model systems to explain aspects of the photophysics of excited states in such polymers and obtain a clear picture of the spatial extent of the singlet and triplet manifolds.[7−12] What is particularly important is that the strong spin−orbit coupling associated with these heavy metals enables significant mixing of singlet and triplet states, which renders the spin-forbidden emission from the triplet excited state (phosphorescence) partially allowed.[7−12] In contrast to hydrocarbon conjugated polymers, the triplet excited state is accessible to experimentation by various optical methods. Significant advances have been realized in this area.[11−13] In earlier work on metal polyynes, a vast range of platinum-containing monomers and polymers have been prepared where alkynyl units are separated by a variety of aromatic ring systems (e.g., phenyl, pyridyl, oligothienyl, anthryl, etc.) with different electronic properties.[11−16]

The synthesis of polymeric derivatives of fluorene (PFs) has recently attracted increasing research attention as an interesting approach to the development of efficient blue-light-emitting polymers.[17−22] The facile functionalization at C-9 imparts an appropriate control of both polymer solubility and potential interchain interactions in films.[23−26] Two major approaches have been employed to enhance the performance of PFs. The use of bulky substituents in the main chain[26] and the deliberate inclusion of conjugation-interrupting groups tend to limit the intrinsic conjugation length in the polymer backbone.[27−32] To depress chain aggregation and increase quantum efficiency, the introduction of disorder to the conjugated system seemed to be an attractive route,[33,34] and Xia et al. have recently reported the decreased aggregation phenomena in PFs by using carbazole copolymer units.[34]

Recently, we are interested in the chemistry and photophysics of new organometallic polyynes incorporating fluorene-based auxiliaries,[35−37] and the first example of a soluble, low-band-gap platinum(II) polyyne polymers with a 9-dicyanomethylenefluorene spacer has been communicated in preliminary form.[37] Along these lines, we report here our strategies in improving the material properties of this class of metal polyynes. We have introduced the 9,9-dihexylfluorene linkage unit through the 2,7-positions into the polymeric platinum alkynyl chain. By virtue of the good hole-transporting abilities of carbazole derivatives to balance the charge injection between the emitting layer and the anode in LEDs,[34,38,39,40] attempts have also been made to incorporate 9-alkyl-substituted carbazole unit via 3,6-positions into our polymer system, and the results are compared and correlated with the corresponding fluorene counterparts (Chart 1). The dependence of the first excited singlet and triplet electronic state on the nature of fluorene units in the bridging ligand will also be discussed in this contribution.

Experimental Section

General. All reactions were carried out under a nitrogen atmosphere with the use of standard Schlenk techniques, but no special precautions were taken to exclude oxygen during workup. Solvents were predried and distilled from appropriate drying agents. All reagents and chemicals, unless otherwise

* Corresponding author: e-mail rwywong@hkbu.edu.hk, Fax (852)2339-7348.

10.1021/ma0117108 CCC: $22.00
Published on Web 03/19/2002

Chart 1[a,b]

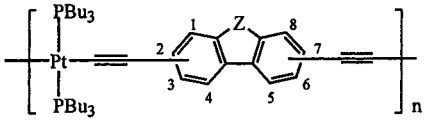

Z = CH_2 **[Pt-TFT]$_\infty$** [a]

$C(C_6H_{13})_2$ **[Pt-T(C_6H_{13}-F)T]$_\infty$** [a]

C=O **[Pt-T(FO)T]$_\infty$** [a]

C=C(H){(C_5H_4)Fe(C_5H_5)} **[Pt-T(Fc-F)T]$_\infty$** [a]

$C=C(CN)_2$ **[Pt-T(CN-F)T]$_\infty$** [a]

$N(C_4H_9)$ **[Pt-T(C_4H_9-C)T]$_\infty$** [b]

[a] Substitution at 2,7-positions. [b] Substitution at 3,6-positions.

stated, were purchased from commercial sources and used without further purification. Preparative TLC was performed on 0.7 mm silica plates (Merck Kieselgel 60 GF_{254}) prepared in our laboratory. The compounds *trans*-[$PtCl(Ph)(PEt_3)_2$][41] and *trans*-[$PtCl_2(PBu_3)_2$][42] were prepared by literature methods. Infrared spectra were recorded as CH_2Cl_2 solutions using a Perkin-Elmer Paragon 1000 PC or a Nicolet Magna 550 series II FTIR spectrometer. NMR spectra were measured in appropriate solvents on a JEOL EX270 or a Varian Inova 400 MHz FT-NMR spectrometer, with ^{1}H and ^{13}C NMR chemical shifts quoted relative to TMS and ^{31}P chemical shifts relative to an 85% H_3PO_4 external standard. Electron impact (EI) and fast atom bombardment (FAB) mass spectra were recorded on a Finnigan MAT SSQ710 mass spectrometer. Electronic absorption spectra were obtained with a HP 8453 UV−vis spectrometer. For emission spectral measurements, the 325 nm line of a He−Cd laser was used as an excitation source. The luminescence spectra were analyzed by a 0.25 m focal length double monochromator with a Peltier cooled photomultiplier tube and processed with a lock-in amplifier. For the low-temperature experiments, samples were mounted in a closed-cycle cryostat (Oxford CC1104) in which the temperature can be adjusted from 10 to 330 K. The fluorescence quantum yields were determined in CH_2Cl_2 solutions at 290 K against the anthracene standard in the same solvent (Φ = 0.27).[43] Cyclic voltammetry experiments were done with a Princeton Applied Research (PAR) model 273A potentiostat. A conventional three-electrode configuration consisting of a glassy-carbon working electrode and a Pt wire as the counter and reference electrodes was used at a scan rate of 100 mV/s. The solvent in all measurements was deoxygenated CH_2Cl_2, and the supporting electrolyte was 0.1 M $[Bu_4N]BF_4$. Ferrocene was added as a calibrant after each set of measurements, and all potentials reported were quoted with reference to the ferrocene−ferrocenium couple. The molecular weights of the polymers were determined by GPC (HP 1050 series HPLC with visible wavelength and fluorescent detectors) using polystyrene standards, and thermal analyses were performed with Shimadzu DSC-50 and Perkin-Elmer TGA6 thermal analyzers. The polymer films for the photocurrent measurements were prepared by casting the polymer solution from 1,1,2,2-tetrachloroethane onto ITO-coated glass substrates. Measurements of the spectral response were made by illuminating the device through the ITO side. Optical excitation was provided by a xenon arc lamp at 400 and 370 nm for [Pt−T(C_6H_{13}−F)T]$_\infty$ and [Pt−T(C_4H_9−C)T]$_\infty$, respectively. The setup for the photoconductivity experiment was described in the literature.[44]

[Pt−T(C_6H_{13}−F)T]$_1$. To a stirred mixture of 2,7-diethynyl-9,9-dihexylfluorene (0.076 g, 0.20 mmol) and 2 equiv of *trans*-[$PtCl(Ph)(PEt_3)_2$] (0.218 g, 0.40 mmol) in ^{i}Pr_2NH (20 mL) and CH_2Cl_2 (20 mL) was added CuI (8 mg). The solution was stirred at room temperature over a period of 15 h, after which all volatile components were removed under vacuum. The crude product was taken up in CH_2Cl_2 and purified on preparative TLC plates with hexane/CH_2Cl_2 (3:2, v/v) as eluent giving the title complex as an oily solid in an isolated yield of 88% (0.246 g). IR (CH_2Cl_2): ν(C≡C) 2091 cm^{-1}. ^{1}H NMR ($CDCl_3$): δ (ppm) 7.44 (d, J = 7.0 Hz, 2H, $H_{4,5}$), 7.34 (d, J = 7.0 Hz, 2H, $H_{3,6}$), 7.25−7.21 (m, 6H, $H_{1,8}$ + H_{ortho} of Ph), 6.96 (t, J = 7.3 Hz, 4H, H_{meta} of Ph), 6.80 (t, J = 7.3 Hz, 2H, H_{para} of Ph), 1.89−1.74 (m, 28H, PCH_2 + $CH_2(CH_2)_4CH_3$), 1.25−1.01 (m, 52H, PCH_2CH_3 + $CH_2(CH_2)_4CH_3$), 0.78 (t, J = 7.3 Hz, 6H, $(CH_2)_5CH_3$). ^{13}C NMR ($CDCl_3$): δ (ppm) 156.26, 150.23, 139.01, 137.98, 129.51, 127.16, 126.97, 125.11, 121.12, 118.59 (arom C), 112.60, 111.47 (C≡C), 54.27 (sp^3-quat. C), 40.29, 31.38, 29.62, 23.46, 22.48, 13.93 (C_6H_{13}), 14.93, 7.93 (Et). ^{31}P {^{1}H} ($CDCl_3$): δ (ppm) 11.12 ($^1J_{P-Pt}$ = 2628 Hz). FAB-MS (*m*/*z*): 1398 [M^+]. Anal. Calcd for $C_{65}H_{102}P_4Pt_2$: C, 55.86; H, 7.36. Found: C, 55.85; H, 7.58.

[Pt−T(C_6H_{13}−F)T]$_\infty$. A mixture of 2,7-diethynyl-9,9-dihexylfluorene (0.115 g, 0.30 mmol) and *trans*-[$PtCl_2(PBu_3)_2$] (0.201 g, 0.30 mmol) in a 1:1 molar ratio in ^{i}Pr_2NH/CH_2Cl_2 (60 mL, 1:1, v/v) was allowed to react in the presence of CuI (6 mg) at room temperature for 15 h. The resulting solution was evaporated to dryness. The residue was redissolved in CH_2Cl_2 and filtered through a silica gel column, eluting with CH_2Cl_2. Upon removal of solvent, an off-white film was obtained, which was then reprecipitated twice from a CH_2Cl_2/MeOH mixture followed by washing with hexane to give an off-white fibrous solid in 82% yield (0.241 g). IR (CH_2Cl_2): ν(C≡C) 2096 cm^{-1}. ^{1}H NMR ($CDCl_3$): δ (ppm) 7.45 (d, J = 8.1 Hz, 2H, $H_{4,5}$), 7.21 (m, 4H, $H_{1,3,6,8}$), 2.30−2.07 (m, 12H, PCH_2), 1.74−1.57 (m, 12H, PCH_2CH_2), 1.52−1.43 (m, 16H, $P(CH_2)_2CH_2$ + $CH_2(CH_2)_4CH_3$), 1.22−0.83 (m, 34H, $P(CH_2)_3CH_3$ + $CH_2(CH_2)_4CH_3$), 0.78 (t, J = 7.0 Hz, 6H, $(CH_2)_5CH_3$). ^{13}C NMR ($CDCl_3$): δ (ppm) 150.27, 138.30, 129.54, 126.87, 125.10, 118.77 (arom C), 110.06, 107.74 (C≡C), 54.49 (sp^3-quat C), 40.74, 31.59, 29.84, 24.11, 22.68, 14.02 (C_6H_{13}), 26.36, 24.44, 23.93, 13.84 (Bu). ^{31}P {^{1}H} ($CDCl_3$): δ (ppm) 4.32 ($^1J_{P-Pt}$ = 2348 Hz). GPC (THF as eluent): M_w = 28 900, M_n = 16 900, polydispersity = 1.71. Anal. Calcd for $(C_{53}H_{86}P_2Pt)_n$: C, 64.94; H, 8.84. Found: C, 65.03; H, 9.10.

[Pt−T(C_4H_9−C)T]$_1$. The dehydrohalogenation reaction of 9-butyl-3,6-diethynylcarbazole (0.054 g, 0.20 mmol) with 2 equiv of *trans*-[$PtCl(Ph)(PEt_3)_2$] (0.218 g, 0.40 mmol), in the presence of CuI (8 mg), in ^{i}Pr_2NH/CH_2Cl_2 (40 mL, 1:1, v/v) afforded the title complex as a white solid in 60% yield (0.155 g) after the usual workup by TLC on silica using CH_2Cl_2/hexane (1:1, v/v) as eluent. IR (CH_2Cl_2): ν(C≡C) 2093 cm^{-1}. ^{1}H NMR ($CDCl_3$): δ (ppm) 8.01 (s, 2H, $H_{4,5}$), 7.43−7.38 (m, 6H, $H_{2,7}$ + H_{ortho} of Ph), 7.20 (d, J = 8.4 Hz, 2H, $H_{1,8}$), 6.99 (t, J = 7.2 Hz, 4H, H_{meta} of Ph), 6.82 (t, J = 7.2 Hz, 2H, H_{para} of Ph), 4.21 (t, J = 7.2 Hz, 2H, NCH_2), 1.85−1.79 (m, 26H, PCH_2 + NCH_2CH_2), 1.39−1.33 (m, 2H, CH_2CH_3), 1.18−1.10 (m, 36H, PCH_2CH_3), 0.93 (t, J = 7.2 Hz, 3H, CH_3). ^{13}C NMR ($CDCl_3$): δ (ppm) 156.74, 139.19, 138.41, 128.76, 127.14, 122.47, 122.29, 121.01, 119.68, 107.95 (arom C), 110.75, 108.56 (C≡C), 42.69, 31.06, 20.43, 13.81 (Bu), 15.02, 7.99 (Et). ^{31}P {^{1}H} ($CDCl_3$): δ (ppm) 10.92 ($^1J_{P-Pt}$ = 2645 Hz). FAB-MS (*m*/*z*): 1286 [M^+]. Anal. Calcd for $C_{56}H_{85}NP_4Pt_2$: C, 52.29; H, 6.66; N, 1.09. Found: C, 52.14; H, 6.30; N, 0.89.

[Pt−T(C_4H_9−C)T]$_\infty$. Polymerization was carried out by mixing 9-butyl-3,6-diethynylcarbazole (0.108 g, 0.40 mmol), *trans*-[$PtCl_2(PBu_3)_2$] (0.268 g, 0.40 mmol), and CuI (8 mg) in ^{i}Pr_2NH/CH_2Cl_2 (80 mL, 1:1, v/v) under nitrogen. After stirring at room temperature for 15 h, the solution mixture was evaporated to dryness. The residue was redissolved in CH_2Cl_2, filtered through a silica column using the same eluent. After removal of the solvent, the crude product was purified by precipitation in CH_2Cl_2 from MeOH. Subsequent washing with hexane and drying in vacuo gave an off-white powder (0.264 g, 76%). IR (CH_2Cl_2): ν(C≡C) 2099 cm^{-1}. ^{1}H NMR ($CDCl_3$): δ (ppm) 7.94 (s, 2H, $H_{4,5}$), 7.40 (d, J = 8.4 Hz, 2H, $H_{2,7}$), 7.20 (d, J = 8.4 Hz, 2H, $H_{1,8}$), 4.22 (t, J = 7.2 Hz, 2H, NCH_2), 2.25−2.21 (m, 12H, PCH_2), 1.84−1.78 (m, 2H, NCH_2CH_2), 1.71−1.67 (m, 12H, PCH_2CH_2), 1.54−1.45 (m, 12H, $P(CH_2)_2CH_2CH_3$), 1.41−1.34 (m, 2H, $N(CH_2)_2CH_2CH_3$), 0.96 (t, J = 7.2 Hz, 21H, CH_3). ^{13}C NMR ($CDCl_3$): δ (ppm) 138.59, 128.89, 122.53, 122.40, 119.59, 108.04 (arom C), 109.36, 107.60 (C≡C), 42.84, 31.14, 20.53, 15.09 (NBu), 26.41, 24.48, 23.95, 13.92 (PBu_3). ^{31}P {^{1}H} ($CDCl_3$): δ (ppm) 4.04 ($^1J_{P-Pt}$ = 2377 Hz). GPC (THF as eluent): M_w = 19 100, M_n = 8920,

Scheme 1. Synthesis of Monomers and Polymers[a]

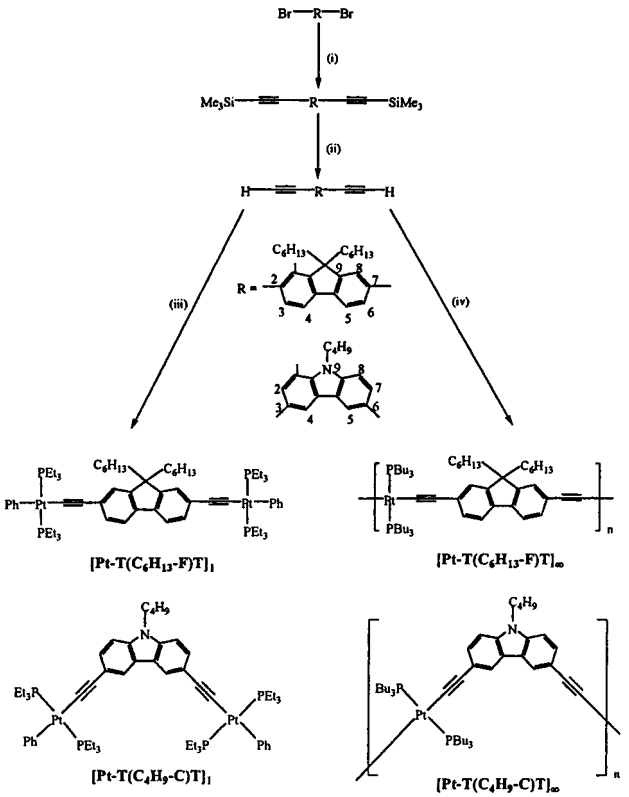

[a] Reagents and conditions: (i) trimethylsilylacetylene, $Pd(OAc)_2$, PPh_3, CuI, $^iPr_2NH$, 75 °C; (ii) K_2CO_3, MeOH, r.t.; (iii) *trans*-$[PtPh(Cl)(PEt_3)_2]$, CuI, $^iPr_2NH$, r.t.; (iv) *trans*-$[PtCl_2(PBu_3)_2]$, CuI, $^iPr_2NH$, r.t.

polydispersity = 2.14. Anal. Calcd for $(C_{44}H_{69}NP_2Pt)_n$: C, 60.81; H, 8.00; N, 1.61. Found: C, 60.55; H, 7.90; N, 1.42.

X-ray Crystallography. Colorless crystals of $[Pt-T(C_4H_9-C)T]_1$ suitable for X-ray diffraction studies were grown by slow evaporation of its solution in hexane at room temperature. Geometric and intensity data were collected using graphite-monochromated Mo Kα radiation (λ = 0.710 73 Å) on a Bruker Axs SMART 1000 CCD area detector. The collected frames were processed with the software SAINT,[45] and an absorption correction was applied (SADABS)[46] to the collected reflections. The structure was solved by direct methods (SHELXTL)[47] in conjunction with standard difference Fourier techniques and subsequently refined by full-matrix least-squares analyses on F^2. All non-hydrogen atoms were assigned with anisotropic displacement parameters. Crystal data: $C_{56}H_{85}NP_4Pt_2$, M = 1286.31, triclinic, space group $P\bar{1}$, a = 18.383(1) Å, b = 19.000(1) Å, c = 19.882(1) Å, α = 116.040(1)°, β = 92.361(1)°, γ = 101.907(1)°, U = 6036.0(7) Å^3, Z = 4, T = 293 K, μ(Mo Kα) = 4.768 mm^{-1}, 35 510 reflections measured, 25 835 unique, R_{int} = 0.0199, final R_1 = 0.0373, wR_2 = 0.0963 for 25 835 [$I > 2\sigma(I)$] observed reflections.

Results and Discussion

Synthesis. Scheme 1 shows the chemical structure and the synthetic route to the monomers and polymers under investigation. The triple bonds are abbreviated by T, fluorene rings by F, and carbazole rings by C. Monomers and polymers are differentiated by use of the subscripts 1 and ∞, respectively. 2,7-Dibromo-9,9-dihexylfluorene was prepared by a slight modification of the literature method[19,34] whereas 3,6-dibromo-9-butylcarbazole was synthesized in quantitative yield starting from 3,6-dibromocarbazole by nucleophilic substitution with bromobutane in the presence of NaH.[40] The Sonogashira coupling sequence of $Me_3SiC{\equiv}CH$ with these dibromo species readily provided the corresponding bis(trimethylsilylethynyl) derivatives in good yields, which, upon desilylation with K_2CO_3 in MeOH, gave the diterminal alkyne compounds $HC{\equiv}CRC{\equiv}CH$ (R = 9,9-dihexylfluorene-2,7-diyl, $H_2T(C_6H_{13}-F)T$, or 9-butylcarbazole-3,6-diyl, $H_2T(C_4H_9-C)T$).[15,35,48,49] The yields of these transformations are high. We note that alkylation at the N atom should proceed first before the CuI-catalyzed coupling reaction in the synthesis of $Me_3SiC{\equiv}CRC{\equiv}CSiMe_3$ (R = 9-butylcarbazole-3,6-diyl), presumably due to instability of the N−H group in an amine solvent. Both ligand precursors $H_2T(C_6H_{13}-F)T$ and $H_2T(C_4H_9-C)T$ can be used to form monomeric and polymeric complexes of platinum by the adaptation of the dehydrohalogenation procedures reported previously using the CuI/$^iPr_2NH$ catalytic system.[37,50] The feed mole ratio of the platinum chloride precursors and the diethynyl ligands were 2:1 and 1:1 for the monomer and polymer syntheses, respectively, and each product was carefully purified to remove ionic impurities and catalyst residues. The monomers $[Pt-T(C_6H_{13}-F)T]_1$ and $[Pt-T(C_4H_9-C)T]_1$ were isolated in fairly good yields by preparative TLC on silica. Purification of the polymers $[Pt-T(C_6H_{13}-F)T]_\infty$ and $[Pt-T(C_4H_9-C)T]_\infty$ was accomplished by silica column chromatography using CH_2Cl_2 as eluent, and they were obtained in high purity and yields (75−80%). All these platinum complexes are air-stable and readily dissolve in aprotic solvents such as THF, CH_2Cl_2, $CHCl_3$, or toluene. The polymers are easily processable from organic solvents and exhibit good film-forming properties. The molecular weights of both polymers were determined in THF by gel permeation chromatography (GPC) using polystyrene as a standard to give the weight- and number-average molecular weights listed in Table 1. Indexes of polydispersity (M_w/M_n) around 2 have been calculated, which is consistent with a polycondensation reaction and the degree of polymerization calculated from M_n ranges from 10 to 17. Similar molecular weight distributions have been observed for other reported platinum(II) polyynes based on the same reference standard.[11,12,37] GPC data indicate that the number of repeat units per chain for $[Pt-T(C_6H_{13}-F)T]_\infty$ is higher than that for $[Pt-T(C_4H_9-C)T]_\infty$, but the degree of polymerization is reduced in both cases as compared to those found for other platinum-containing fluorene-based materials (Chart 1).[35−37]

Table 1. Structural and Thermal Properties of the Polymers

polymer	M_w	M_n	M_w/M_n	T_g (°C)	T_{decomp} (onset) (°C)
$[Pt-T(C_6H_{13}-F)T]_\infty$	28 900	16 900	1.71	83 ± 3	349 ± 5
$[Pt-T(C_4H_9-C)T]_\infty$	19 100	8 920	2.14	95 ± 4	315 ± 5

Chemical Characterization. The IR, NMR (^1H, ^{13}C and ^{31}P), MS, and elemental analysis data shown in the Experimental Section are in accordance with the chemical structures of our samples and are similar to other platinum ethynylfluorene polymers recently prepared.[35−37] The IR spectra of these new platinum(II) complexes display a single sharp ν(C≡C) absorption at ca. 2091−2099 cm^{-1}, which together with the singlet signal observed in each $^{31}P\{^1H\}$ NMR spectrum reveal a trans geometry of the $Pt(PR_3)_2$ (R = Et or Bu) unit in these square-planar monomeric and polymeric materials. The ν(C≡C) stretching frequencies for $[Pt-T(C_6H_{13}-F)T]_\infty$ and $[Pt-T(C_4H_9-C)T]_\infty$ are lower than those for the free ligand precursors $H_2T(C_6H_{13}-F)T$ and H_2T-

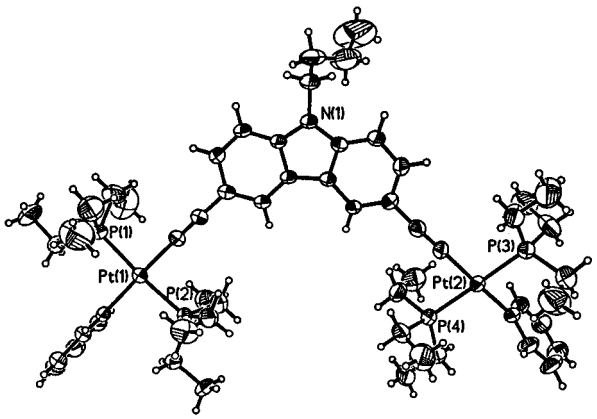

Figure 1. A perspective drawing of $[Pt-T(C_4H_9-C)T]_1$ with the ellipsoids shown at the 25% probability level. Labels on the carbon atoms and all hydrogen atoms have been omitted for clarity.

$(C_4H_9-C)T$, in line with a higher degree of conjugation in the former. The $^1J_{P-Pt}$ values range from 2628 to 2645 Hz for the monomers and 2348−2377 Hz for the polymers, typical of those for related *trans*-PtP_2 systems.[35−37,51,52] The formulas of $[Pt-T(C_6H_{13}-F)T]_1$ and $[Pt-T(C_4H_9-C)T]_1$ were also established by appearance of the intense molecular ion peaks in the respective positive FAB mass spectra. NMR analyses clearly indicate that a well-defined structure has been obtained in each compound. In all cases, ^{1}H NMR resonances arising from the protons of the organic moieties were observed. Notably, two distinct ^{13}C NMR signals for the individual sp carbons in these monomers and polymers were observed, in accord with their formulations, and they are shifted downfield with respect to the free ligands. The aromatic region of their ^{13}C NMR spectra also gives more precise information about the regiochemical structure of the main-chain skeleton and reveals a high degree of structural regularity in the polymers. As an example, only 10 well-defined peaks appear in the aromatic region, related to the 20 aromatic carbon atoms of the symmetric diplatinum structure for $[Pt-T(C_6H_{13}-F)T]_1$. The resonances due to the butyl and ethyl groups are clearly identified and the characteristic peak at about 54.3 ppm corresponds to the sp^3-carbon atom of the fluorene moiety. Similarly, the ^{13}C NMR spectral features of $[Pt-T(C_6H_{13}-F)T]_\infty$ and $[Pt-T(C_4H_9-C)T]_\infty$ agree with the polymer structures shown. The exact three-dimensional solid-state structure of $[Pt-T(C_4H_9-C)T]_1$ has been confirmed by a single-crystal X-ray analysis (Figure 1). Important bond distances and angles are given in Table 2. The coordination geometry at each Pt center is square-planar with the two PEt_3 groups trans to each other, and both metal end groups are bridged by a 9-butylcarbazolediyl-spaced bis(acetylide) ligand via 3,6-positions. To our knowledge, this is the first structurally characterized example of a carbazole-linked platinum−alkynyl complex. The C≡C bond length [average 1.213(7) Å] is characteristic of metal−acetylide σ bonding,[15,36] and the central carbazole ring is essentially planar. The average bond angle of 176.0(6)° for the fragment Pt−C≡C conforms to the rigid-rod nature of the monomer. There is no apparent intermolecular interactions of note in its crystal lattice.

Electrochemistry. The electrochemical nature of our compounds was investigated in CH_2Cl_2 by cyclic voltammetry (Table 3). Within the measured scan range, only two irreversible oxidation waves were observed for the monomers $[Pt-T(C_6H_{13}-F)T]_1$ and $[Pt-T(C_4H_9-C)T]_1$, attributable to the stepwise two-electron oxidation at the platinum center $[Pt^{2+} \rightarrow Pt^{3+} + e^- \rightarrow Pt^{4+} + 2e^-]$. Similar redox processes have been encountered for the blue platinum(II) diynes with the diethynylthieno[3,4-*b*]pyrazine moiety.[53] The polymers $[Pt-T(C_6H_{13}-F)T]_\infty$ and $[Pt-T(C_4H_9-C)T]_\infty$ only display a single irreversible oxidation wave at about +0.40 and +0.27 V, respectively, corresponding to the one-electron oxidation of the metal residue. The first oxidation potential was shown to be slightly more anodic for the monomers than for the polymers.

Thermal Analysis. The thermal properties of both polymers were examined by thermal gravimetry (TG) and differential scanning calorimetry (DSC) under nitrogen (Table 1). Analysis of the TG trace (heating rate 20 °C/min) for $[Pt-T(C_6H_{13}-F)T]_\infty$ and $[Pt-T(C_4H_9-C)T]_\infty$ shows that they have decomposition temperatures in excess of 300 °C, indicative of good thermal stability. Our results indicate that decomposition starts at 349 and 315 °C for $[Pt-T(C_6H_{13}-F)T]_\infty$ and $[Pt-T(C_4H_9-C)T]_\infty$, respectively. The onset of decomposition is very similar for $[Pt-T(C_6H_{13}-F)T]_\infty$ and $[Pt-T(CN-F)T]_\infty$ (ca. 352 °C),[37] but $[Pt-T(C_4H_9-C)T]_\infty$ has a lower decomposition temperature, consistent with the recent observation that the carbazole unit can exert a disorder effect on the PFs system. We note a 42% weight loss between 350 and 545 °C for $[Pt-T(C_6H_{13}-F)T]_\infty$ whereas 46% of the weight is lost between 315 and 515 °C for $[Pt-T(C_4H_9-C)T]_\infty$. The decomposition step can be assigned to the removal of two PBu_3 groups from the polymers. The glass transition temperatures (T_g) were found to be 83 and 95 °C for $[Pt-T(C_6H_{13}-F)T]_\infty$ and $[Pt-T(C_4H_9-C)T]_\infty$, respectively, which are lower than those in other fluorene derivatives of this class.[36,37] Apparently, the determined T_g values are comparable with those of 9,9-dialkyl-substituted polyfluorenes,[26] hyperbranched polycarbazoles,[39] poly(9-tetradecanyl-3,6-(dibutadiynylcarbazole)),[39] and some poly(2,7-9,9-dioctylfluorene) polymers with or without carbazole units.[34] Another endotherm observed at 213 and 200 °C may be attributed to the melting of $[Pt-T(C_6H_{13}-F)T]_\infty$ and $[Pt-T(C_4H_9-C)T]_\infty$, respectively. The polymer $[Pt-T(C_6H_{13}-F)T]_\infty$ also shows an additional exothermic phase transition at ca. 137 °C.

Optical Absorption Spectroscopy. Optical absorption spectra of the polymers and corresponding monomers were taken at room temperature in CH_2Cl_2 solutions and as thin films. Relevant data are gathered in Table 3. For $[Pt-T(C_6H_{13}-F)T]_1$ and $[Pt-T(C_6H_{13}-F)T]_\infty$, they display similar structured ligand-localized $\pi-\pi^*$ absorption bands in CH_2Cl_2 in the range 307−399 nm. Each of the carbazole derivatives $[Pt-T(C_4H_9-C)T]_1$ and $[Pt-T(C_4H_9-C)T]_\infty$ essentially shows three absorption peaks in the near-UV region (ca. 258−344 nm) due to $\pi-\pi^*$ transitions of the bridging ligand. We associate the lowest energy absorption peak with the $S_0 \rightarrow S_1$ transition from the highest occupied molecular orbital (HOMO) to the lowest unoccupied molecular orbital (LUMO), which are delocalized π- and π^*-orbitals. As compared to the band peaking at 330 nm for the free ligand $H_2T(C_6H_{13}-F)T$, we find that the position of the lowest energy absorption band is red-shifted when the platinum group is introduced, i.e., on going from $H_2T(C_6H_{13}-F)T$ to $[Pt-T(C_6H_{13}-F)T]_1$ and $[Pt-T(C_6H_{13}-F)T]_\infty$. A similar bathochromic shift of

Table 2. Selected Bond Lengths (Å) and Angles (deg) for [Pt−T(C$_4$H$_9$−C)T]$_1$

	molecule 1	molecule 2		molecule 1	molecule 2
Pt(1)−P(1)	2.268(2)	2.273(2)	Pt(1)−P(2)	2.272(2)	2.287(2)
Pt(2)−P(3)	2.284(2)	2.280(2)	Pt(2)−P(4)	2.282(2)	2.280(2)
Pt(1)−C(19)	2.021(6)	1.999(6)	Pt(2)−C(38)	2.010(6)	2.018(6)
C(19)−C(20)	1.209(7)	1.234(7)	C(20)−C(21)	1.424(8)	1.425(8)
C(37)−C(38)	1.221(7)	1.189(7)	C(26)−C(37)	1.433(8)	1.429(8)
P(1)−Pt(1)−P(2)	174.89(6)	174.73(7)	P(1)−Pt(1)−C(19)	88.7(2)	89.4(2)
P(2)−Pt(1)−C(19)	86.4(2)	87.5(2)	P(3)−Pt(2)−P(4)	175.15(7)	176.65(7)
P(3)−Pt(2)−C(38)	92.0(2)	88.7(2)	P(4)−Pt(2)−C(38)	85.5(2)	88.0(2)
Pt(1)−C(19)−C(20)	178.0(6)	174.7(6)	C(19)−C(20)−C(21)	177.0(7)	179.3(7)
Pt(2)−C(38)−C(37)	172.6(6)	178.7(6)	C(26)−C(37)−C(38)	176.8(7)	176.7(7)

Table 3. Absorption, Emission, and Redox Data for the Monomers and Polymers

	λ_{max} (nm)			λ_{em} (nm)[f]				
	CH_2Cl_2[a]	film	E_g (eV)[b]	CH_2Cl_2 (290 K)[c]	film (290 K)	film (11 K)	$\Delta E(T_1 \rightarrow S_0, S_1 \rightarrow S_0)$[d]	E_{ox} (V)[e]
[Pt−T(C$_6$H$_{13}$−F)T]$_1$	309 (0.2)	311	3.12	411 (0.30)	396*, 418, 552, 598*	396*, 418*, 554, 604*	6.6	+0.46
	358 (1.0)	359						+0.70
	376 (1.4)	378						
[Pt−T(C$_6$H$_{13}$−F)T]$_\infty$	307 (0.4)	309	2.92	421, 555* (0.01)	432, 552*	416*, 433*, 554, 589*, 606*	18.0	+0.40
	399 (2.9)	404						
[Pt−T(C$_4$H$_9$−C)T]$_1$	260 (4.1)	263	3.36	410*, 426 (0.48)	408*, 426	407*, 425*, 459, 474*	11.0	+0.30
	304 (2.1)	304						+0.78
	333 (3.7)	343						
[Pt−T(C$_4$H$_9$−C)T]$_\infty$	258 (9.2)	261	3.10	412*, 428 (0.01)	404*, 427	403*, 426*, 462, 497*, 511*	136.0	+0.27
	301 (4.0)	304						
	344 (7.0)	347						

[a] Extinction coefficients are shown in parentheses. [b] Estimated from the onset wavelength of the solid-state optical absorption. [c] Fluorescence quantum yields shown in parentheses are measured in CH_2Cl_2 relative to anthracene. [d] Ratio of the intensities of triplet emission to singlet emission at 11 K. [e] Irreversible waves. [f] Asterisks indicate emission peaks appear as shoulders or weak bands.

absorption maximum was also observed for the carbazole analogue (from 302 to 333 and 344 nm). This reveals that π-conjugation of the ligands extends into and through the metal center, consistent with the previous results on related systems.[11,15] In the same way, the transition energies of the polymers are lowered with respect to those of the corresponding monomers, suggesting that the first optical absorption transition in the polymers arises from an electronic excitation that is delocalized over more than one monomer unit.[12] This agrees with the results of other materials of this class having pyridine, phenylene, or thiophene spacer[12] but is in contrast to [Pt−T(CN−F)T]$_\infty$ where the lowest singlet excited state is only confined to a single repeat unit.[37] It is worthwhile to compare the band gap values of a series of fluorene-functionalized platinum(II) polyynes demonstrating different electronic characteristics. In energy terms, the HOMO−LUMO energy gap (E_g) as measured from the onset wavelength in solid film state is 2.92 eV for [Pt−T(C$_6$H$_{13}$−F)T]$_\infty$ and 3.10 eV for [Pt−T(C$_4$H$_9$−C)T]$_\infty$, which are larger than those in other fluorene-based materials (Table 4).[35−37] According to the identity of the Z unit, the optical gap of these polyynes follows the experimental order N(C$_4$H$_9$) > C(C$_6$H$_{13}$)$_2$ ≥ CH$_2$ > C═O ≈ C═C(H){(C$_5$H$_4$)Fe(C$_5$H$_5$)} > C═C(CN)$_2$. With reference to the parent fluorene derivative [Pt−TFT]$_\infty$, we note that the 9-dicyanomethylene group enhances conjugation while both C(C$_6$H$_{13}$)$_2$ and N(C$_4$H$_9$) units reduce conjugation in the present system. Hence, the energy of the S_1 singlet state depends significantly on the nature of the Z moiety of the ring and is highest for the 9-butylcarbazole and 9,9-dihexylfluorene cases. These facts attest to the importance of tuning the electronic properties of the central fluorene ring in governing the efficiency of intersystem crossing $S_1 \rightarrow T_1$ (vide infra).

Table 4. Optical Data of Platinum(II) Fluorene- and Carbazole-Based Materials

polymer	color	S_0-S_1 transition in CH_2Cl_2 (nm)	E_g (eV)	ref
[Pt−TFT]$_\infty$	off-white	394	2.90	35
[Pt−T(C$_6$H$_{13}$−F)T]$_\infty$	off-white	399	2.92	this work
[Pt−T(FO)T]$_\infty$	red	506	2.10	35
[Pt−T(Fc-F)T]$_\infty$	red	437[a]	2.10	36
[Pt−T(CN−F)T]$_\infty$	blue	660	1.58	37
[Pt−T(C$_4$H$_9$−C)T]$_\infty$	off-white	344	3.10	this work

[a] Broad shoulders.

Photoluminescence Spectroscopy. Table 3 lists the emission data of the monomers and polymers in the solution and in the solid states. At 290 K, all of them emit in the blue region ranging from 411 to 428 nm in CH_2Cl_2 solutions and from 418 to 432 nm in solid films. Analogous to the absorption spectra, these emission features are shifted to longer wavelengths from monomers to polymers. Upon gradual cooling, two main emission bands appear in each case. For [Pt−T(C$_6$H$_{13}$−F)T]$_\infty$, we attribute the feature peaking at 433 nm to emission from singlet excited state (fluorescence $S_1 \rightarrow S_0$) at 11 K, due to the small Stokes' shift (ca. 0.20 eV) between the bands in the absorption and the emission spectra (Figure 2).[11] The fluorescence quantum yields measured in CH_2Cl_2 at 290 K for the monomers lie in the range 0.30−0.48, and the lower values associated with their polymeric counterparts are of the same order of magnitude as other reported Pt σ-acetylide polymers.[14] At 11 K, the intense feature at the low-energy regime of the emission spectrum of [Pt−T(C$_6$H$_{13}$−F)T]$_\infty$

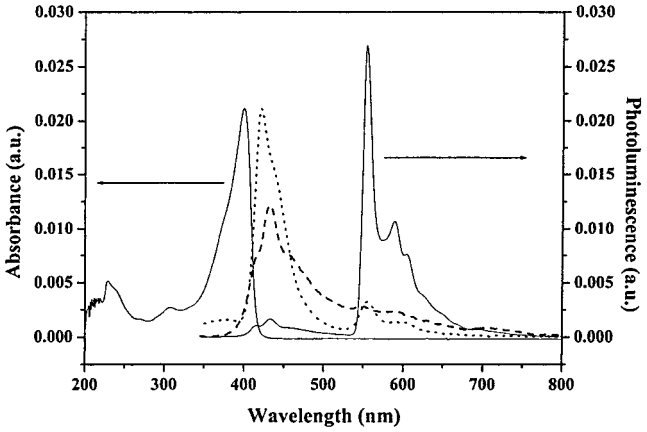

Figure 2. Room temperature optical absorption spectrum and the photoluminescence (PL) spectrum (11 K) of $[Pt-T(C_6H_{13}-F)T]_\infty$ in solid (solid line). The dotted and the dashed lines correspond to the PL spectra in CH_2Cl_2 solution and solid film at 290 K, respectively.

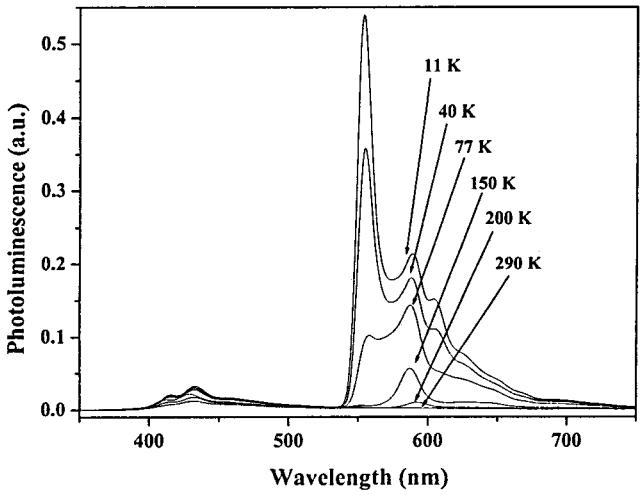

Figure 3. Temperature dependence of the PL of $[Pt-T(C_6H_{13}-F)T]_\infty$.

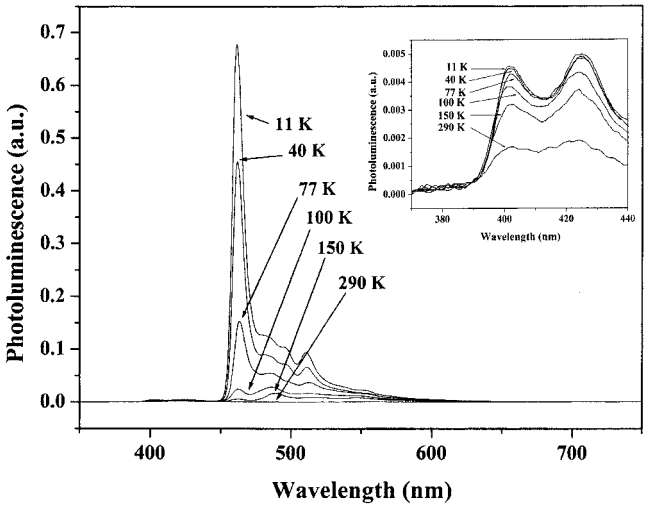

Figure 4. Temperature dependence of the PL of $[Pt-T(C_4H_9-C)T]_\infty$. The inset depicts the weak singlet emissive peaks as a function of temperature.

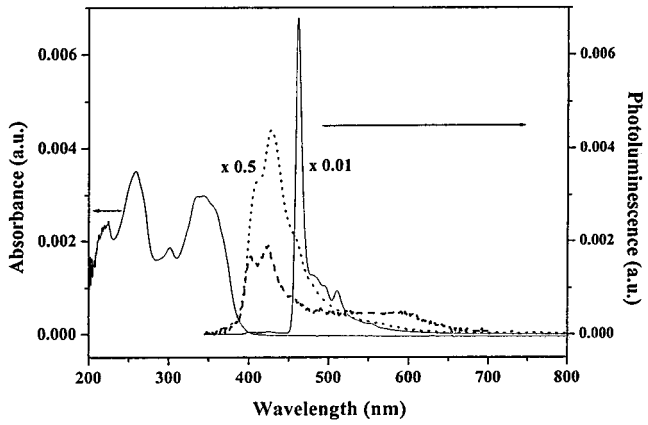

Figure 5. Room temperature optical absorption spectrum and the PL spectrum (11 K) of $[Pt-T(C_4H_9-C)T]_\infty$ in solid (solid line). The dotted and the dashed lines correspond to the PL spectra in CH_2Cl_2 solution and solid film at 290 K, respectively.

with the maximum at around 554 nm is due to emission from a triplet excited state (phosphorescence $T_1 \rightarrow S_0$), and such a triplet emission shows a vibronic structure at low temperature that is typical of this class of materials.[11] The large energy shift observed between absorption and emission features (about 1.0 eV) ascertains this emitting state as a T_1 excited state (Figure 2). This assignment can be further interpreted in terms of the observed temperature dependence of the emission data, in accordance with earlier work on oligothienyl-spaced platinum polyynes.[11] The photoluminescence spectra of both polymers as a function of temperature are shown in Figures 3 and 4. The triplet emission is found to be strongly temperature dependent in contrast to the singlet emission. From 150 to 11 K, the singlet emission peak intensity increases only by a factor of 1.3 for $[Pt-T(C_6H_{13}-F)T]_\infty$. However, the intensity of the lower-lying emission increases by a factor of 63.5, and such an increase in emission intensity indicates a long-lived excited state that is quenched by thermally activated diffusion to dissociation sites at room temperature.[7,11,13] The emission pattern for $[Pt-T(C_4H_9-C)T]_\infty$ is similarly analyzed to consist of a $S_1 \rightarrow S_0$ transition at 426 nm and a $T_1 \rightarrow S_0$ peak at the lower energy side (462 nm) with a large Stokes' shift of ca. 0.9 eV for the latter (Figure 5). In this case, the intensity of the singlet and triplet photoluminescence bands increases by a factor of 1.4 and 68.0, respectively, as the temperature is lowered from 150 to 11 K. These triplet emissive peaks were observed at 554 and 459 nm for the monomers $[Pt-T(C_6H_{13}-F)T]_1$ and $[Pt-T(C_4H_9-C)T]_1$, respectively (Figures 6 and 7). In these systems, the lowest triplet excited state remains strongly localized, as can be inferred from the small energy difference between triplet emissions in the monomers and in the polymers. To evaluate the relative efficiency of intersystem crossing triggered by the heavy metals in our systems, the peak height ratio from triplet emission to singlet emission at 11 K, ΔE ($T_1 \rightarrow S_0$, $S_1 \rightarrow S_0$), was taken as a good indicator (Table 3).[12] Clearly, the intersystem crossing rate is higher for the polymers than that for the monomers in each system. In particular, for $[Pt-T(C_4H_9-C)T]_\infty$ we observe an unusually high efficiency of triplet emission. These data provide an important insight of the effect of the fluorene substituents in improving the efficiency of intersystem crossing in these polyynes. Our investigations indicate that there is no evidence of detecting any $T_1 \rightarrow S_0$ transitions over the measured range for $[Pt-T(FO)T]_\infty$,[54] $[Pt-T(Fc-F)T]_\infty$,[36,54] and $[Pt-T(CN-F)T]_\infty$[11] even at 11 K. The intensity of such a triplet emission is also weak for the parent polymer $[Pt-TFT]_\infty$.[54] One noteworthy

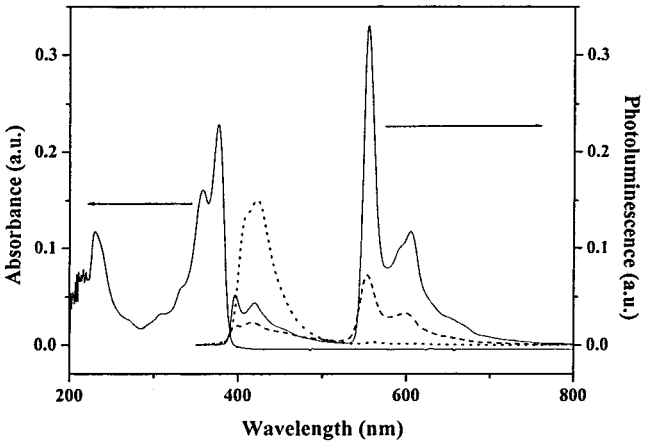

Figure 6. Room temperature optical absorption spectrum and the PL spectrum (11 K) of $[Pt-T(C_6H_{13}-F)T]_1$ in solid (solid line). The dotted and the dashed lines correspond to the PL spectra in CH_2Cl_2 solution and solid film at 290 K, respectively.

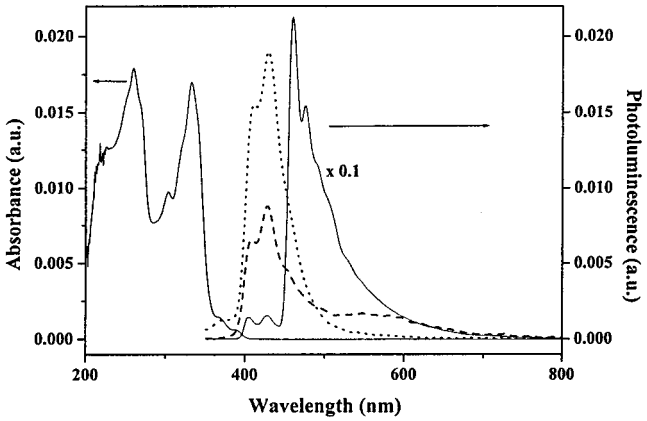

Figure 7. Room temperature optical absorption spectrum and the PL spectrum (11 K) of $[Pt-T(C_4H_9-C)T]_1$ in solid (solid line). The dotted and the dashed lines correspond to the PL spectra in CH_2Cl_2 solution and solid film at 290 K, respectively.

feature here is that a reduction in the HOMO−LUMO band gap leads to a lowering of the intersystem crossing efficiency, and hence the principal emission arises from a $S_1 \rightarrow S_0$ transition. This implies that reduced conjugation in these 9-anchored biphenyl structures effectively facilitates intersystem crossing, and phosphorescence can easily be measured. The use of conjugation-interrupting segments such as $N(C_4H_9)$ and $C(C_6H_{13})_2$ groups in the polymer main chain can control the effective conjugation length and offers a good way to enhance the intersystem crossing rate, especially at low temperatures.

Photocurrent Measurements. Fabrication of the ITO/$[Pt-T(C_6H_{13}-F)T]_\infty$/Al and ITO/$[Pt-T(C_4H_9-C)T]_\infty$/Al photocells (ITO = indium−tin oxide) was carried out for the polymer samples in order to study their photoconductive properties. The experiment was performed by using a lock-in-amplifier to measure the voltage drop across a resistor resulting from the photocurrent through the polymer film. In this way, the signal due to the dark current can be eliminated. The photoconducting behavior of our new polymers was demonstrated, and Figure 8 depicts the logarithmic plots of the photocurrent of both photocells against the applied electric field across the polymer for illumination through the ITO anode. The photocurrent of the devices is field-dependent, and it increases with increasing bias voltage. The curve is steeper at higher voltages, typical of other known organometallic photoconductors.[55] Both polymeric materials show a photocurrent quantum yield of approximately 0.01% at 400 and 370 nm for $[Pt-T(C_6H_{13}-F)T]_\infty$ and $[Pt-T(C_4H_9-C)T]_\infty$, respectively, which is a common value for single layer devices.[11] There is no significant difference in the quantum efficiency with variation of the central fluorene structure, and a similar quantum yield was also determined for the $[Pt-T(FO)T]_\infty$ counterpart.[54]

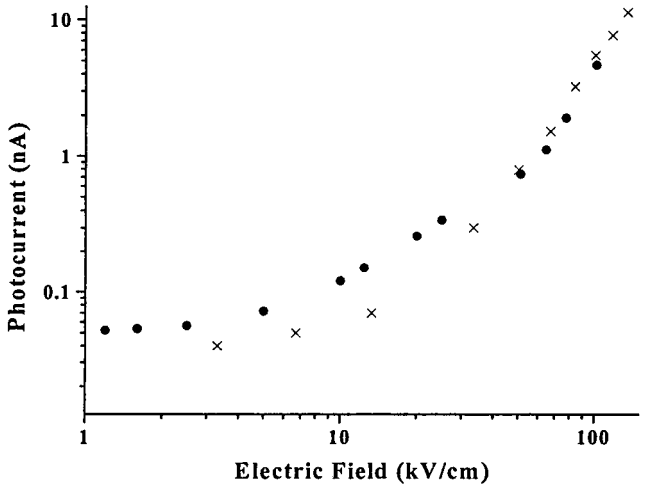

Figure 8. Photocurrent vs external electric field logarithmic plots for $[Pt-T(C_6H_{13}-F)T]_\infty$ (●) and $[Pt-T(C_4H_9-C)T]_\infty$ (×).

Concluding Remarks

As a continuation of our earlier studies on the nature of photoexcited states in organometallic conjugated polymers as a function of π-conjugation in the bridging ligand, a group of soluble, well-defined platinum-containing diyne and polyyne materials consisting of 9,9-dihexylfluorene and 9-butylcarbazole linking units was prepared and fully characterized. The polymers exhibit good thermal stability and photoconducting properties. Our present work demonstrated that by a deliberate incorporation of these 9,9-disubstituted fluorene and 9-alkylcarbazole moieties one can enhance the intersystem crossing efficiency induced by the platinum unit and thus study the phosphorescence process readily. In both systems, the S_1 singlet state is delocalized over several repeat units, but the T_1 triplet state is strongly localized. A systematic correlation was made between the effective conjugation length (or conversely, band gap) and the intersystem crossing rate in these polyynes. The larger the band gap, the higher the efficiency of triplet emission. We believe that the non-π-conjugated sp^3-carbon of fluorene or nitrogen of carbazole is an effective conjugation interrupter in order to limit the conjugation length in the resulting materials. These polymers represent suitable model systems to investigate the relationship between chemical structure and the evolution of singlet and triplet excited states, and the results contribute to our understanding of the structure−property relationship in this class of organometallic conjugated polymers. Work is still in progress to modify the substituents at C-9 or develop new fluorene−heterocycle hybrid monomers in an attempt to achieve better optical performance. Further investigations of LEDs incorporating these materials are currently underway.

Acknowledgment. We are grateful to the Hong Kong Research Grants Council (Grant HKBU 2022/99P)

and the Hong Kong Baptist University for financial support. We also thank Dr. K. W. Cheah at the Hong Kong Baptist University and Dr. W. K. Chan at the University of Hong Kong for the access of their research facilities to perform the photoluminescence and photocurrent measurements, respectively.

Supporting Information Available: Preparations of ligand precursors, temperature-dependent emission spectra of the monomers, and tables of X-ray crystal data. This material is available free of charge via the Internet at http://pubs.acs.org.

References and Notes

(1) *Conjugated Polymeric Materials: Opportunities in Electronics, Optoelectronics and Molecular Electronics*; Brédas, J. L., Chance, R. R., Eds.; Kluwer Academic Publishers: Dordrecht, 1990.
(2) Burroughes, J. H.; Bradley, D. D. C.; Brown, A. R.; Marks, R. N.; Mackay, K.; Friend, R. H.; Burn, P. L.; Holmes, A. B. *Nature (London)* **1990**, *347*, 539.
(3) Tessler, N.; Denton, G. J.; Friend, R. H. *Nature (London)* **1996**, *382*, 695.
(4) Halls, J. J. M.; Walsh, C. A.; Greenham, N. C.; Marseglia, E. A.; Friend, R. H.; Moratti, S. C.; Holmes, A. B. *Nature (London)* **1995**, *376*, 498.
(5) Yu, G.; Gao, J.; Hummelen, J. C.; Wudl, F.; Heeger, A. J. *Science* **1995**, *270*, 1789.
(6) Brown, A. R.; Bradley, D. D. C.; Burroughes, J. H.; Friend, R. H.; Greenham, N. C.; Burn, P. L.; Holmes, A. B.; Kraft, A. *Appl. Phys. Lett.* **1992**, *61*, 2793.
(7) Wittmann, H. F.; Friend, R. H.; Khan, M. S.; Lewis, J. *J. Chem. Phys.* **1994**, *101*, 2693.
(8) Beljonne, D.; Wittmann, H. F.; Köhler, A.; Graham, S.; Younus, M.; Lewis, J.; Raithby, P. R.; Khan, M. S.; Friend, R. H.; Brédas, J. L. *J. Chem. Phys.* **1996**, *105*, 3868.
(9) Wittmann, H. F.; Fuhrmann, K.; Friend, R. H.; Khan, M. S.; Lewis, J.; *Synth. Met.* **1993**, *55-57*, 56.
(10) Köhler, A.; Wittmann, H. F.; Friend, R. H.; Khan, M. S.; Lewis, J. *Synth. Met.* **1994**, *67*, 245.
(11) Chawdhury, N.; Köhler, A.; Friend, R. H.; Wong, W. Y.; Lewis, J.; Younus, M.; Raithby, P. R.; Corcoran, T. C.; Al-Mandhary, M. R. A.; Khan, M. S. *J. Chem. Phys.* **1999**, *110*, 4963.
(12) Chawdhury, N.; Köhler, A.; Friend, R. H.; Younus, M.; Long, N. J.; Raithby, P. R.; Lewis, J. *Macromolecules* **1998**, *31*, 722.
(13) Köhler, A.; Wittmann, H. F.; Friend, R. H.; Khan, M. S.; Lewis, J. *Synth. Met.* **1996**, *77*, 147.
(14) Khan, M. S.; Kakkar, A. K.; Long, N. J.; Lewis, J.; Raithby, P.; Nguyen, P.; Marder, T. B.; Wittmann, F.; Friend, R. H. *J. Mater. Chem.* **1994**, *4*, 1227.
(15) Lewis, J.; Long, N. J.; Raithby, P. R.; Shields, G. P.; Wong, W. Y.; Younus, M. *J. Chem. Soc., Dalton Trans.* **1997**, 4283.
(16) Kingsborough, R. P.; Swager, T. M. *Prog. Inorg. Chem.* **1999**, *48*, 123.
(17) Janietz, S.; Bradley, D. D. C.; Grell, M.; Giebeler, C.; Inbasekaran, M.; Woo, E. P. *Appl. Phys. Lett.* **1998**, *73*, 2453.
(18) Grice, A. W.; Bradley, D. C. C.; Bernius, M. T.; Inbasekaran, M.; Wu, W. W.; Woo, E. P. *Appl. Phys. Lett.* **1998**, *73*, 629.
(19) Yu, W.-L.; Pei, J.; Cao, Y.; Huang, W.; Heeger, A. J. *Chem. Commun.* **1999**, 1837.
(20) Klärner, G.; Davey, M. H.; Chen, W.-D.; Scott, J. C.; Miller, R. D. *Adv. Mater.* **1998**, 993.
(21) Ranger, M.; Rondeau, D.; Leclerc, M. *Macromolecules* **1997**, *30*, 7686.
(22) Pschirer, N. G.; Bunz, U. H. F. *Macromolecules* **2000**, *33*, 3961.
(23) Lemmer, U.; Heun, S.; Mahrt, R. F.; Scherf, U.; Hopmeir, M.; Siegner, U.; Göbel, R. O.; Mullen, K.; Bassler, H. *Chem. Phys. Lett.* **1995**, *240*, 373.
(24) Grüner, J.; Wittmann, H. F.; Hamer, P. J.; Friend, R. H.; Huber, J.; Scherf, U.; Müllen, K.; Moratti, S. C.; Holmes, A. B. *Synth. Met.* **1994**, *67*, 181.
(25) Jenekhe, S. A.; Osaheni, J. A. *Science* **1994**, *265*, 765.
(26) Kreyenschmidt, M.; Klaerner, G.; Fuhrer, T.; Ashenhurst, J.; Karg, S.; Chen, W. D.; Lee, V. Y.; Scott, J. C.; Miller, R. D. *Macromolecules* **1998**, *31*, 1099.
(27) Fáber, R.; Stasko, A.; Nuyken, O. *Macromol. Chem. Phys.* **2000**, *201*, 2257.
(28) Malliaras, G. G.; Herrema, J. K.; Wildeman, J.; Wieringa, R. H.; Gill, R. E.; Lampoura, S. S.; Hadziioannou, G. *Adv. Mater.* **1993**, *5*, 721.
(29) Hilberer, A.; van Hutten, P. F.; Wildeman, J.; Hadziioannou, G. *Macromol. Chem. Phys.* **1997**, *198*, 2211.
(30) Remmers, M.; Schulze, M.; Wegner, G. *Macromol. Rapid Commun.* **1996**, *17*, 239.
(31) Martínez, A. G.; Barcina, J. O.; Cerezo, A. de F.; Schlüter, A.-D.; Frahn, J. *Adv. Mater.* **1999**, *11*, 27.
(32) Pei, Q.; Yang, Y. *Chem. Mater.* **1995**, *7*, 1568.
(33) Son, S.; Dodabalapur, A.; Lovinger, A. J.; Galvin, M. E. *Science* **1995**, *269*, 376.
(34) Xia, C.; Advincula, R. C. *Macromolecules* **2001**, *34*, 5854.
(35) Lewis, J.; Raithby, P. R.; Wong, W. Y. *J. Organomet. Chem.* **1998**, *556*, 219.
(36) Wong, W. Y.; Wong, W. K.; Raithby, P. R. *J. Chem. Soc., Dalton Trans.* **1998**, 2761.
(37) Wong, W. Y.; Choi, K. H.; Lu, G. L.; Shi, J. X. *Macromol. Rapid Commun.* **2001**, *22*, 461.
(38) Wang, C.; Yuan, C.; Wu, H.; Wei, Y. *J. Appl. Lett.* **1995**, *78*, 4264.
(39) Tao, X.-T.; Zhang, Y.-D.; Wada, T.; Sasabe, H.; Suzuki, H.; Watanabe, T.; Miyata, S. *Adv. Mater.* **1998**, *10*, 226.
(40) Maruyama, S.; Zhang, Y.; Wada, T.; Sasabe, H. *J. Chem. Soc., Perkin Trans. 1* **1999**, 41.
(41) Chatt, J.; Shaw, B. L. *J. Chem. Soc.* **1960**, 4020.
(42) Chatt, J.; Hayter, R. G. *J. Chem. Soc., Dalton Trans.* **1961**, 896.
(43) Dawson, W. R.; Windsor, M. W. *J. Phys. Chem.* **1968**, *72*, 3251.
(44) Ng, W. Y.; Chan, W. K. *Adv. Mater.* **1997**, *9*, 716.
(45) *SAINT, Reference Manual*; Siemens Energy and Automation: Madison, WI, 1994−1996.
(46) Sheldrick, G. M. *SADABS, Empirical Absorption Correction Program*; University of Göttingen: Germany, 1997.
(47) Sheldrick, G. M. *SHELXTL, Reference Manual*, ver. 5.1, Madison, WI, 1997.
(48) Sonogashira, K.; Tohda, Y.; Hagihara, N. *Tetrahedron Lett.* **1975**, 4467.
(49) Takahashi, S.; Kuroyama, Y.; Sonogashira, K.; Hagihara, N. *Synthesis* **1980**, 627.
(50) Takashahi, S.; Kariya, M.; Yatake, T.; Sonogashira, K.; Hagihara, N. *Macromolecules* **1978**, *11*, 1063.
(51) Long, N. J.; Martin, A. J.; Vilar, R.; White, A. J. P.; Williams, D. J.; Younus, M. *Organometallics* **1999**, *18*, 4261.
(52) Wong, W. Y.; Chan, S. M.; Choi, K. H.; Cheah, K. W.; Chan, W. K. *Macromol. Rapid Commun.* **2000**, *21*, 453.
(53) Younus, M.; Köhler, A.; Cron, S.; Chawdhury, N.; Al-Mandhary, M. R. A.; Khan, M. S.; Lewis, J.; Long, N. J.; Friend, R. H.; Raithby, P. R. *Angew. Chem., Int. Ed.* **1998**, *37*, 3036.
(54) Wong, W. Y.; Choi, K. H., unpublished work.
(55) Chakraborty, A. K.; Bhattacharjee, A.; Mallik, B. *Bull. Chem. Soc. Jpn.* **1994**, *67*, 607.

MA0117108